A Section 508–conformant HTML version of this article is available at https://doi.org/10.1289/EHP2594.

Projecting Age-Stratified Risk of Exposure to Inland Flooding and Wildfire Smoke in the United States under Two Climate Scenarios

David Mills,[1] Russell Jones,[1] Cameron Wobus,[1] Julia Ekstrom,[2] Lesley Jantarasami,[3] Alexis St. Juliana,[1] and Allison Crimmins[4]

[1]Abt Associates, Boulder, Colorado, USA
[2]Policy Institute for Energy, Environment and the Economy, University of California, Davis, California, USA
[3]Oregon Department of Energy, Salem, Oregon, USA
[4]U.S. Environmental Protection Agency, Washington, DC, USA

Background: The public health community readily recognizes flooding and wildfires as climate-related health hazards, but few studies quantify changes in risk of exposure, particularly for vulnerable children and older adults.

Objectives: This study quantifies future populations potentially exposed to inland flooding and wildfire smoke under two climate scenarios, highlighting the populations in particularly vulnerable age groups (≤4 y old and ≥65 y old).

Methods: Spatially explicit projections of inland flooding and wildfire under two representative concentration pathways (RCP8.5 and RCP4.5) are integrated with static (2010) and dynamic (2050 and 2090) age-stratified projections of future contiguous U.S. populations at the county level.

Results: In both 2050 and 2090, an additional one-third of the population will live in areas affected by larger and more frequent inland flooding under RCP8.5 than under RCP4.5. Approximately 15 million children and 25 million older adults could avoid this increased risk of flood exposure each year by 2090 under a moderate mitigation scenario (RCP4.5 compared with RCP8.5). We also find reduced exposure to wildfire smoke under the moderate mitigation scenario. Nearly 1 million young children and 1.7 million older adults would avoid exposure to wildfire smoke each year under RCP4.5 than under RCP8.5 by the end of the century.

Conclusions: By integrating climate-driven hazard and population projections, newly created county-level exposure maps identify locations of potential significant future public health risk. These potential exposure results can help inform actions to prevent and prepare for associated future adverse health outcomes, particularly for vulnerable children and older adults. https://doi.org/10.1289/EHP2594

Introduction

Human health threats from climate change are occurring both in the United States (Melillo et al. 2014; USGCRP 2016) and globally (Costello et al. 2009; Patz et al. 2014; Watts et al. 2015). The public health community consistently identifies changes in extreme events as a key driver of climate health impacts, with the majority of publications focusing on heat waves (Verner et al. 2016) and coastal storms and flooding (Bell et al. 2016). Inland flooding and wildfires are comparatively understudied in the climate impacts literature, although they have well-known direct and indirect adverse public health outcomes, including increased mortality and morbidity (Bell et al. 2016; Liu et al. 2017; Reid et al. 2016; Terti et al. 2017). Because climate change will lead to continued increases in these extreme events in the United States (Wehner et al. 2017; Bell et al. 2016), there is a need for prospective national-level analyses to better understand the spatial distribution of exposure. Such analyses should aim to dynamically assess future risk and account for change over time in climatic, socioeconomic, and demographic factors (Jurgilevich et al. 2017).

Inland flooding and wildfires each present distinct health risks, which can vary over time (i.e., before, during, or after an event) and distance from the event. Examples of flood health risks include drowning, injuries, electrocution, motor vehicle accidents, increased disease or infections from contaminated water, and mental health impacts (Bell et al. 2016; 2017). Wildfire health risks include worsened air quality from smoke exposure that can exacerbate respiratory and cardiovascular conditions, watershed changes and erosion that can degrade water quality, and mental health impacts (Bell et al. 2016; 2017).

Although any exposure to these extreme events increases a person's potential for experiencing an adverse health outcome, certain groups within exposed populations are more vulnerable because they have increased sensitivity or less adaptive capacity (or both) than others. Specifically, children and older adults are among those most vulnerable to the health effects of floods and wildfire (Al-Rousan et al. 2014; English and Richardson 2016; Gamble et al. 2016; Haq 2017; Rappold et al. 2017). Both children's and older adults' respiratory systems are more physically sensitive to particulate matter pollution from wildfire smoke, contributing to increased risk of hospitalization and, for older adults, increased risk of death (Bell et al. 2013; Delfino et al. 2009; Gamble et al. 2016; Liu et al. 2017; Perera 2017). Both children and older adults have greater risk of gastrointestinal illness and severe health outcomes from contact with contaminated water, a common result of exposure to a flood (Trtanj et al. 2016). Those ≥65 y old tend to have a lower capacity to cope and prepare for impacts of extreme events than younger adults given their higher rates of chronic illness, reduced mobility, greater isolation, and less financial flexibility (English and Richardson 2016; Meyer 2017). Both the very young and older adults are also more vulnerable to extreme events because their exposure is often determined or influenced by the preparation and response of their caregivers (Gamble et al. 2016). In addition, severe extreme events or those that occur simultaneously or in succession in a given location have the potential to overwhelm the coping mechanisms of an individual or community, creating additional vulnerability (Bell et al. 2016; Ebi and Bowen 2016).

We estimated future populations within the contiguous United States (CONUS) exposed to projected changes in two inland flooding metrics and one wildfire smoke metric. We developed spatially explicit projections of exposure to inland floods and wildfire smoke by integrating data from multiple global climate models

Address correspondence to A. Crimmins, U.S. EPA, 1200 Pennsylvania Ave., NW (6207-A), Washington, DC, 20460. Telephone: 202.343.9170. Email: crimmins.allison@epa.gov

The authors declare they have no actual or potential competing financial interests.

Received 1 August 2017; Revised 23 February 2018; Accepted 7 March 2018; Published 17 April 2018.

(GCMs) under two climate scenarios in the mid- (2040–2059) and late (2080–2099) 21st century with county-specific projections of U.S. populations for 2050 and 2090. To isolate the impact of the projected changes in these events, we also estimated future impacts using a static 2010 population level and distribution. We present results for populations exposed to extreme events separately for the very young (≤4 y old), older adults (≥65 y old), and all ages. This study contributes to the relatively small, but growing, body of literature that provides quantitative estimates of future population exposure to climate health threats. It is also one of the first national-level analyses for the United States that compares multiple extreme event types under two climate futures and presents age-stratified results to characterize future populations at risk of exposure.

Methods

Climate Change Projections

Consistent with the U.S. Environmental Protection Agency's (U.S. EPA's) Climate Change Impacts and Risk Analysis (CIRA) project (U.S. EPA 2017a), our wildfire analysis incorporates data from a subset of five GCMs selected from among those used in the fifth Coupled Model Intercomparison Project ensemble (CMIP5) (Taylor et al. 2012). These five GCMs (CCSM4, GISS-E2-R, CanESM2, HadGEM2-ES, and MIROC5) capture much of the variability observed across the CMIP5 ensemble and have localized constructed analogs (LOCAs) downscaling available for the contiguous United States (see Table S1 for details). The LOCA downscaled results from these GCMs are used as inputs to the MC2 model that projects future acreage burned by wildfire in our analyses.

When selecting climate models from the broader ensemble for the wildfire analysis, we compared projections from CMIP5 GCMs for annual and seasonal temperature and precipitation. Although these averaged metrics may not be perfect substitutes for comparing extreme weather effects, the relationship was assumed to be sufficiently strong for this purpose. The five GCMs selected capture a large range of the variability across the entire ensemble in terms of annual and seasonal temperature and precipitation (see Figures S1–S3), account for model independence and demonstrate skill at reproducing observed climate at the global scale (Sanderson et al. 2015a, 2015b), and are broadly used by the scientific community.

Our inland flooding analysis draws on downscaled and consistently formatted hydrological outputs from 29 GCMs in CMIP5 (U.S. Department of the Interior, 2014; Mizukami et al. 2016; Wobus et al. 2017). The flooding analysis considers a larger sample of GCMs than the wildfire analysis to increase the statistical power of sampling for the low-probability flood events of interest.

The inland flooding and wildfire modeling incorporate temperature and precipitation data from two representative concentration pathways (RCPs) for each GCM that reflect alternative future climates. Identified by their approximate total radiative forcing in the year 2100 relative to the year 1750 (in watts per square meter), the two pathways are RCP8.5, which reflects a scenario with continued high greenhouse gas (GHG) emissions growth, and RCP4.5, which reflects a scenario with moderate global GHG emissions growth. Under RCP8.5, by 2100, global atmospheric carbon dioxide (CO_2) levels rise from current-day levels of approximately 400 parts per million (ppm) to 936 ppm, with a projected warming of approximately 4°C (2.8–5.7°C), by 2081–2100. Under RCP4.5, projections show atmospheric CO_2 levels at the end of the century remain below 550 ppm, leading to a warming of approximately 2°C (1.3–3.3°C) by the end of the century (USGCRP 2017a).

To provide localized climate projections and to bias correct the projections to improve consistency with the historical period, we used the LOCA data set [Pierce et al., 2014, 2015; U.S. Department of the Interior et al., 2016]. The LOCA projections, which are derived from the CMIP5 ensemble outputs, are the primary data set used in the Climate Science Special Report of the U.S. Global Change Research Program's Fourth National Climate Assessment (USGCRP 2017b). The LOCA downscaled data set provides daily maximum and minimum temperatures (T_{min} and T_{max}), and daily precipitation values at 1/16-degree resolution from 2006 to 2100. For each climate scenario, we calculated an average daily change factor for temperature and precipitation at each grid cell by comparing 20 y of LOCA projections centered on 2050 and 2090 to an historical 1/16-degree gridded data set from the period 1986–2005 (Livneh et al., 2015). We calculated these daily change factors as a spatial average of nine 1/16-degree LOCA grid cells (3×3 window) surrounding each location.

We calculated hourly temperature change factors based on model-projected changes in T_{min} and T_{max} by assuming these temperatures occur at midnight and noon, respectively, and interpolating between T_{min} and T_{max} values over the course of each day. These hourly changes were then added to the baseline North American Land Data Assimilation System (NLDAS) temperature time series. For precipitation, we used the GCM outputs to calculate a multiplier to apply to the hourly NLDAS precipitation time series. In some cases, the LOCA-modeled precipitation led to unrealistically high change factors. To eliminate these outliers, we first discarded values that exceeded the 90th percentile of all change factors for each station. Daily change factors were then calculated as a 31-d moving average ratio of this filtered time series and were applied to the NLDAS baseline.

Projecting Changes to Inland Flooding

For our inland flooding analysis, we captured changes in both the frequency and magnitude of high flow events with a 1% annual exceedance probability (AEP) threshold (referred to as a 1% AEP flood). This threshold is a common metric for evaluating extreme flooding, most notably because the 1% AEP or "100-y" flood level delineates Special Flood Hazard Areas in federal flood insurance rate maps (FEMA 2017). Within observed or modeled data, a 1% AEP flood defines both a flow volume (e.g., 10,000 cubic feet per second) and an expected return interval or frequency for that flow volume (on average, once every 100 y).

We developed inland flooding projections using downscaled hydrologic data developed over the past decade by the U.S. Bureau of Reclamation and a broad group of collaborators (U.S. Department of the Interior 2014). These hydrologic data used GCM-modeled outputs for precipitation and temperature downscaled by the bias correction and spatial disaggregation method (Wood et al. 2004; Wood and Mizukami 2014). The resulting adjusted precipitation and temperature fields were then used as inputs to a variable infiltration capacity hydrologic model to simulate catchment hydrology (Liang et al. 1994). Runoff from this model was remapped to the Hydrologic Response Units (HRUs) defined in the United States Geological Survey Geospatial Fabric (Viger and Bock 2014) and routed through the Geospatial Fabric river network using the MizuRoute routing tool (Mizukami et al. 2016). The U.S. Reclamation. (2014) provides additional details of the downscaling, hydrologic projections, and catchment hydrology simulations. This modeling does not address coastal flooding from ocean storms because different models (e.g., storm surge models)

and data (e.g., sea level rise data) would be required to project this type of flooding event (U.S. EPA, 2017a).

The hydrologic outputs from the U.S. Reclamation. (2014) include projections of naturalized daily flow (i.e., flow without dams) through the 21st century at approximately 57,000 stream reaches in the United States. For each of these stream reaches, we extracted the modeled time series of annual maximum flows for the entire 21st century (2001–2099) from each of the 29 GCMs and 2 RCPs. We then fit a generalized extreme value distribution to the annual maximum flow time series using the pooled data from the 29 GCMs for each RCP at three 20-y intervals referenced by their midpoint: a 2010 baseline (2001–2020), 2050 (2040–2059), and 2090 (2080–2099). Although individual GCMs are not strictly statistically independent owing to shared code (e.g., Knutti et al., 2010; Bishop and Abramowitz, 2013), the consensus of the climate modeling community remains that it is best to average across many ensemble members. Accordingly, our estimate of the 1% AEP flow relied on a full ensemble of GCM projections (e.g., Tebaldi and Knutti 2007). Wobus et al. (2017) provide additional details of the statistical methods applied to estimate changes in the frequency of baseline 1% AEP flow and the magnitude of the flows for the 1% AEP flood over time. Further discussion of methodological choices, implications of pooling data from multiple GCMs, and uncertainty around internal variability can be found in the supplementary information in Wobus et al. (2017).

Using these data, we considered changes in the frequency of flows consistent with the historical 1% AEP flood based on available modeled data for a baseline period (i.e., the baseline 1% AEP flood). This change in frequency is expressed as a new return interval for the flow associated with the baseline 1% AEP flood. We also considered changes in the magnitude of the 1% AEP flow. This change in magnitude was captured by comparing the flow for the 1% AEP flood calculated based on future projections to the flow for the baseline 1% AEP flood.

Figure 1 provides an example of how we used projected flow information from each river reach to measure changes in the frequency and magnitude of 1% AEP flows.

Projecting Changes to Wildfires

We projected acreage burned by wildfires using the MC2 dynamic global vegetation model (DGVM) developed for the CIRA project (U.S. EPA 2017a). MC2 is a spatially explicit DGVM with three integrated modules that address biogeography, biogeochemistry, and fire (OSU 2011). MC2 accounts for potential impacts of a future climate, primarily temperature and precipitation data developed in GCMs, on a user-defined and calibrated baseline vegetation layer. The model is calibrated using historical observed climate, vegetation, and biogeographic data as input into the model, then compared to natural vegetation from a historical vegetation map of the same time period.

Recent research investigated the differences between statistical and dynamic vegetation modeling approaches and found that including changes in vegetation and drought–fire dynamics yields potentially important distinctions for projections of long-term changes in fire regimes (Hantson et al. 2016; McKenzie and Littell 2017). The MC2 model simulates changes in future terrestrial ecosystem vegetative cover, including shifts in vegetative type, growth, decay, and transition over time. MC2's fire module incorporates algorithms that account for vegetation characteristics (e.g., type, volume, moisture content) to determine when fire occurs in a grid cell (see Bachelet et al. 2015 for additional detail). Over the century-long modeled period, an area can potentially burn multiple times if there is enough growth of combustible fuel and if projected environmental conditions satisfy ignition criteria. However, MC2 also captures the potential impact of repeated burning resulting in conversion to vegetation types that burn less frequently. Thus, areas with large levels of current wildfire activity may see fewer wildfires in the future in MC2 projections than in a statistical model.

We used results for each of the five GCMs for each year in midcentury (2040–2059) and late-century (2080–2099) 20-y time periods under both RCP8.5 and RCP4.5. MC2 reports the impacts of fire as the percent of the grid cell area burned, among other metrics, where grid cells are $1/16^{\circ}$ resolution. Because the model does not provide a measurement of wildfire smoke emissions, concentrations, or dispersion, we used the percent of the grid cell burned metric to link wildfire frequency to populations potentially exposed to associated smoke [see "Integrating Wildfire and Population Projections" (below) for a description of the calculation of wildfire smoke exposure]. We considered only wildfire smoke distribution to calculate spatially gridded exposure frequency, omitting consideration of potential spatial distribution of other wildfire health impacts, such as threats to water quality or mental health. Risk of exposure to these important health impacts are only captured inasmuch as they occur in the grid cells projected to experience a wildfire year.

Projecting Changes to U.S. Populations

We used county-level data from the U.S. EPA's Integrated Climate and Land Use Scenarios (ICLUSv2) project (U.S. EPA 2017b) to determine the total number of persons that could be exposed to future inland flooding and wildfire smoke. ICLUSv2 projects CONUS populations using the median variant projection

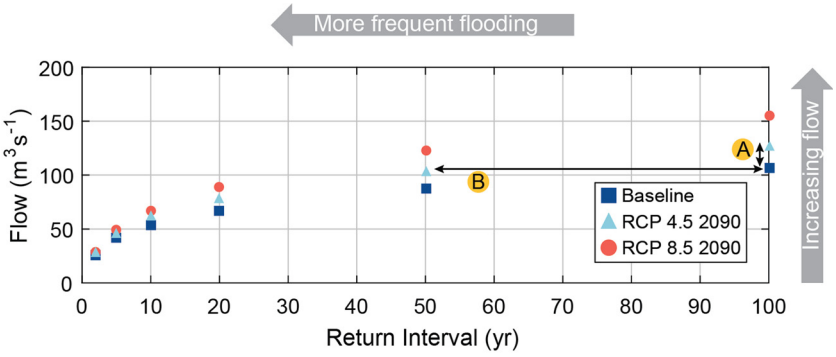

Figure 1. Example of change in inland flooding for one river reach. In this example, the flow for a flood with a baseline 100-y return interval [1% annual exceedance probability (AEP) event] becomes approximately 25% larger (vertical shift from 100 to 125 $m^3 s^{-1}$, marked "A") in 2090 under RCP4.5. At the same time, the 100 $m^3 s^{-1}$ flow that defines the baseline 1% AEP flood becomes approximately twice as frequent (horizontal shift from 100-y to 50-y average return interval, marked "B") in 2090 under RCP4.5. RCP, representative concentration pathway.

of the United Nations' 2015 World Population Prospects data set (United Nations 2015). This scenario represents a midrange national population projection (≈ 440 million people by 2090), which is reasonable given recent demographic trends in the United States (Hollmann et al. 2000). The spatial pattern of population change in ICLUSv2 is dependent on underlying assumptions regarding fertility, migration rate, and international immigration. The proportions of the all-age population in each county for those ≤4 y old and ≥65 y old from the first version of ICLUS were applied to the ICLUSv2 all-age county populations to calculate equivalent county-based age-group-based populations for the years 2010, 2050, and 2090.

Integrating Inland Flooding and Population Projections

Once the flooding projections were calculated for each of the 57,000 CONUS stream reaches, we aggregated these projections to the county level to link them to the population projections. To do this, we intersected all of the stream reaches in the United States with county boundaries and calculated county-average changes in frequency and magnitude for the baseline 1% AEP flood for each combination of future reporting year and RCP.

Flood frequency. For projected changes in flood frequency, we averaged the projected future return intervals of all reaches within each county to calculate a county-averaged change in the recurrence interval of the baseline 1% AEP flood:

$$FRI_{100} = \frac{100}{RI_{avg}}, \quad (1)$$

where

FRI_{100} = the future 100-y flood return interval index, and

RI_{avg} = the county-average future return interval for the baseline 1% AEP flood for the given combination of reporting year and RCP.

County FRI_{100} values >1.0 indicate that, on average, the modeled reaches intersecting the county would experience the baseline 1% AEP flood more frequently in the future. In the example depicted in Figure 1, a county FRI_{100} value of 2 under RCP4.5 in 2090 would indicate that reaches intersecting the county are projected to experience the baseline 1% AEP flow roughly twice as frequently, or every 50 y on average, compared with every 100 y in the baseline period.

Flood magnitude. We followed a similar process to develop a county-level measure of the anticipated change in the magnitude of the 1% AEP flow over time. First, for each modeled reach intersecting a county, we calculated the flow for the 1% AEP event for each combination of future reporting year and RCP. We then calculated a future flow index as follows:

$$FFI_{100} = \frac{FF_{100}}{BF_{100}}, \quad (2)$$

where

FFI_{100} = the future 1% AEP flow index,

FF_{100} = the magnitude of flow for a 1% AEP event for the given combination of future year and RCP, and

BF_{100} = the magnitude of flow for a baseline 1% AEP event.

Finally, we averaged the FFI_{100} values for all reaches intersecting the county to produce the county-average FFI_{100} value for the representative year and RCP. The resulting county-average FFI_{100} values provide an indexed measure of the anticipated relative change in the magnitude of the flows for a 1% AEP event in each future time period relative to the baseline. In the example depicted in Figure 1, a county-average FFI_{100} value of 1.25 for 2090 under RCP4.5 would indicate that the flow for the future 1% AEP flood event is 25% larger than in the baseline. Similarly, county-average FFI_{100} values ≤1 would reflect future 1% AEP flows of the same size or smaller than the baseline 1% AEP event.

We used the ICLUSv2 county-level age-group population projections for 2050 and 2090 to summarize the populations exposed to different categories of anticipated change in the frequency of baseline 1% AEP floods and the magnitude of 1% AEP flows over time. We made the simplifying assumption that all county residents would experience uniform changes in exposure to future flooding in ways that both directly (e.g., flood waters in homes or businesses) or indirectly (e.g., disruption of services) threaten human health. This assumption does not imply that all county residents will be uniformly affected by changes in flooding (i.e., that they would all uniformly become ill); in fact, research shows that socially vulnerable populations within an affected area experience greater adverse health effects (Cutter et al. 2000; Zahran et al. 2008). The results presented are projections of risk of exposure, not cases of morbidity or mortality. If the outcome of interest in this analysis were property damage, the assumption that all county residents would experience changes in exposure uniformly, instead of only inundated areas within the county, would be an overestimation. But because flooding impacts can create widespread public health threats before, during, and after flooding events (e.g., disruption of communication, transportation, water and electrical services; restricted access to health care; injuries related to evacuation, cleanup, or recovery activities; see Bell et al. 2016), we feel this assumption is appropriate as a metric of change in exposure to health risks.

Different GCMs have different spatial patterns of future hydrologic change that cannot be extracted from the integrated ensemble; therefore, variability by GCM in populations exposed to anticipated changes in the frequency and magnitude of flooding is not shown. However, Wobus et al. (2017) found no systematic differences in results in the annual maximum peak flow magnitudes from the 29 individual GCMs.

Integrating Wildfire and Population Projections

We identified populations potentially exposed to wildfire smoke by first integrating the MC2 output grid with land characteristic data from ICLUSv2. MC2 cells where the ICLUSv2 data indicate that >10% of the total MC2 cell area is classified as a combination of agricultural or urban land were removed from consideration as cells that could burn. In the remaining MC2 cells for each GCM/RCP combination, we summed the number of years when ≥6% (≈500 acres) of the MC2 cell is projected to burn within each 20-y modeling period to characterize wildfire frequency (number of years out of 20 in which the threshold level of burning occurred). The MC2 model captures the implications on future vegetation from differences in fires that burn 6% or 99% of an MC2 cell area, but this difference is not captured by smoke exposure estimates even though wildfires that burn 99% of a grid cell are likely to have broader smoke plumes and higher exposure than those that burn 6% of the cell. Although wildfire smoke may be transported large distances from the event (Bell et al. 2016), MC2 does not model smoke dispersion. Therefore, we made the assumption that only residents in the burning MC2 cell and in the eight surrounding cells would be exposed to the wildfire smoke and would thus be exposed to health risks. The number of years a population in a cell would be exposed to wildfire smoke in each future 20-y modeling period was thus defined by the cell within the 9-cell grid with the maximum number of years when ≥6% of the cell burned. For example, people living in a cell projected to experience 2 wildfire years out of 20 in a future period but who live adjacent to a cell projected to experience 3 wildfire years would be reported to experience 3 wildfire years out of 20 in that period.

To transcribe frequency of wildfires at the grid cell level to population exposed to wildfire smoke at the county level, ICLUSv2 county-level age group populations were distributed evenly over the county area and intersected with the MC2 cell grid to develop population projections for each MC2 cell. These projections were aggregated to county populations and summarized by age group, future representative year, GCM, and RCP, according to the calculated years of potential wildfire smoke exposure, categorized as 1–3, 4–6, or ≥7 y out of the 20 maximum possible years of exposure. County-level data were aggregated to state-level population exposure estimates and then averaged across the five GCMs to produce the reported population exposed for each combination of age category, future year, and RCP.

Our wildfire analysis shows that much of the projected burning occurs in the western states and Great Plains consistently across the five GCMS; there is variation among GCMs in the upper Midwest, Northeast, and Southeast regions (see Figure S4). For example, the number of years out of 20 projected to burn in Florida in 2090 under RCP8.5 differs between the CCSM4 model (many cells with burning) and the HadGEM2-ES model (almost no cells with burning). Additional variation occurs for the results in Texas running south from the panhandle using the MIROC5 data (many cells with burning) and the results from the CAN-ESM2 data (far fewer cells with burning). Although we acknowledge the importance of model variability, we averaged population exposure projections from each of the models for a given time period and RCP because this provides a reasonable basis on which to estimate the extent of future populations exposed to wildfire smoke.

Regional Aggregation of Results

To facilitate the presentation of summaries and comparison of results, we aggregated our exposed population results to the same climate regions used in the forthcoming fourth National Climate Assessment (NCA4) (USGCRP 2017b) (see Figure S5 for a map of the NCA4 regions; see also Table S2 for a list of states included in each NCA4 region).

Results

Climate Change Impacts on the Return Interval for Baseline 1% AEP Floods

As shown in Figure 2, baseline 1% AEP floods are projected to become ≤10 times more frequent in some counties (deep red)

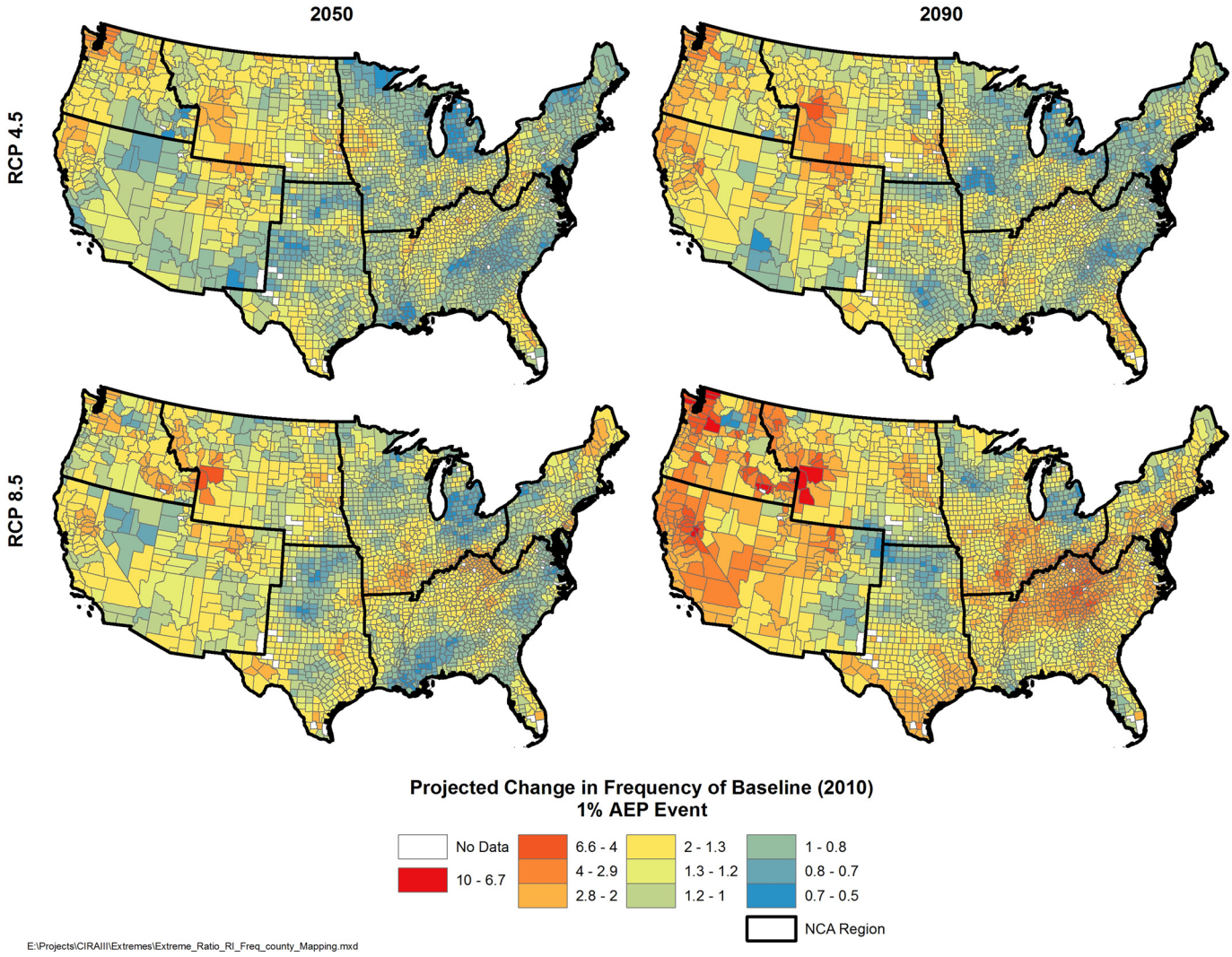

Figure 2. Projected change in the frequency of baseline 1% annual exceedance probability (AEP) floods. Future county-level average future 100-y flood return interval index (FRI_{100} ratios to the 2010 baseline 1% AEP floods are shown under RCP4.5 and RCP8.5 in 2050 and 2090. The most extreme increases in frequency for the baseline flood (values greater than 1) are presented in deep red while the largest decreases in frequency (values less than 1) are presented in dark blue. RCP, representative concentration pathway.

but only half as frequent in others (dark blue) across the two climate scenarios and two future time periods. In all scenarios, more counties are projected to experience an increase than a decrease in frequency of baseline 1% AEP floods, with this trend increasing over time. Under RCP4.5 in 2050, roughly 65% of counties would experience the baseline 1% AEP flood more frequently, increasing to 76% of the counties in 2090. Under RCP8.5, the number of counties experiencing more frequent baseline 1% AEP floods increases from 76% in 2050 to 89% in 2090. These results also show a general trend across the representative years, with the largest anticipated increases in frequency of the baseline 1% AEP flood in the Northwest, Northern Great Plains, and Southwest regions. Simultaneously, there are areas where the baseline 1% AEP floods are expected to occur less frequently in the future across scenarios (e.g., parts of Nebraska and Oklahoma in the Southern Great Plains, and Michigan and Minnesota in the Midwest region).

Projections show that more people will experience more frequent baseline 1% AEP floods than less frequent floods in both 2050 and 2090 and under both RCP4.5 and RCP8.5, in almost every region (Table 1; see Table S3 for state-level results). The only exceptions are in the Midwest and Northeast regions for 2050 under the RCP4.5 scenario. For projections of a given year, more people will live in counties that experience baseline 1% AEP floods more frequently under RCP8.5 than under the RCP4.5 scenario. For projections of a given RCP, more people will live in counties that experience less frequent baseline 1% AEP floods in 2050 than in 2090 despite increasing populations throughout the century. Of particular note is the significantly higher number of people projected to live in counties that experience 1% AEP floods twice as frequently in 2090 under RCP8.5 than under any other year/RCP scenario.

Subtracting the number of children ≤4 y old projected to experience less-frequent flooding in 2050 from the number of children projected to experience floods equally or more frequently than the baseline, we find that a net total of 11.3 million more children live in counties that experience an increase in 1% AEP flood frequency under RCP8.5 than under the RCP4.5 scenario (Table 1). Similarly, a total of 25.8 million more adults ≥65 y old live in counties that experience an increase in 1% AEP flood frequency under RCP8.5 than under the RCP4.5 scenario in 2050. By 2090, the difference between net populations experiencing an increase in baseline 1% AEP flood frequency under RCP8.5 and RCP4.5 increases to 15.1 million children ≤4 y old and 27.2 million adults ≥65 y old. In other words, 15.1 million young children and 27.2 million older adults would avoid increases in baseline 1% AEP flood frequency under RCP4.5 than under RCP8.5 each year by the end of the century. However, despite a

Table 1. Populations affected by changes in the frequency of baseline 1% AEP floods (millions of persons).

	Two or more times more frequently			No change up to 2 times more frequently			Less frequently		
NCA region	Age 0–4	Age ≥65	All ages	Age 0–4	Age ≥65	All ages	Age 0–4	Age ≥65	All ages
RCP4.5 in 2050									
Northeast	0.04	0.02	0.32	2.41	4.87	25.40	3.75	8.04	40.04
Southeast	0.08	0.29	0.98	3.90	9.46	43.39	3.53	8.71	39.47
Midwest	0.05	0.06	0.51	2.93	5.66	31.11	3.62	7.11	38.05
Northern Great Plains	0.07	0.18	0.84	0.50	1.04	5.39	0.02	0.03	0.18
Southern Great Plains	0.00	0.00	0.02	3.62	7.67	37.05	0.67	1.54	7.26
Southwest	0.11	0.34	1.29	6.47	13.84	65.66	1.14	2.43	11.51
Northwest	0.51	1.18	5.59	0.70	1.51	7.50	0.07	0.14	0.70
Total	0.87	2.08	9.56	20.53	44.06	215.50	12.79	28.00	137.21
RCP4.5 in 2090									
Northeast	0.00	0.00	0.01	4.55	8.20	45.35	2.65	4.47	26.23
Southeast	0.67	1.54	7.08	5.92	11.26	59.84	2.55	5.32	26.43
Midwest	0.03	0.04	0.29	4.37	7.01	42.61	3.22	5.03	31.47
Northern Great Plains	0.22	0.48	2.35	0.47	0.77	4.64	0.04	0.05	0.38
Southern Great Plains	0.04	0.06	0.34	3.75	6.86	36.57	1.59	3.15	16.01
Southwest	0.52	1.28	5.48	8.21	14.90	79.30	0.98	1.86	9.62
Northwest	0.81	1.57	8.25	0.61	1.12	6.10	0.06	0.10	0.54
Total	2.29	4.97	23.80	27.88	50.11	274.41	11.09	19.98	110.68
RCP8.5 in 2050									
Northeast	0.40	0.89	4.32	4.45	9.31	47.17	1.35	2.74	14.28
Southeast	0.44	0.89	4.61	4.78	12.01	53.59	2.29	5.56	25.64
Midwest	0.37	0.78	4.02	3.20	6.36	33.69	3.04	5.68	31.97
Northern Great Plains	0.05	0.14	0.60	0.51	1.07	5.52	0.03	0.05	0.28
Southern Great Plains	0.54	1.22	5.65	3.39	7.18	34.76	0.36	0.82	3.92
Southwest	0.17	0.59	2.03	7.52	15.90	76.02	0.03	0.13	0.42
Northwest	0.30	0.63	3.20	0.92	2.08	10.00	0.06	0.11	0.59
Total	2.27	5.14	24.42	24.76	53.90	260.75	7.16	15.09	77.10
RCP8.5 in 2090									
Northeast	2.34	4.03	23.18	4.67	8.34	46.49	0.20	0.30	1.92
Southeast	3.57	6.41	35.51	5.12	10.70	53.02	0.46	1.02	4.82
Midwest	2.30	3.70	22.32	3.38	5.16	32.80	1.94	3.22	19.25
Northern Great Plains	0.14	0.28	1.46	0.52	0.89	5.23	0.07	0.13	0.68
Southern Great Plains	2.81	5.06	27.14	2.05	4.02	20.53	0.52	1.00	5.25
Southwest	7.78	14.09	75.11	1.60	3.27	16.04	0.33	0.68	3.27
Northwest	1.33	2.53	13.50	0.11	0.21	1.09	0.03	0.05	0.30
Total	20.27	36.09	198.21	17.45	32.59	175.20	3.54	6.40	35.49

Note: AEP, annual exceedance probability; NCA, National Climate Assessment; RCP, representative concentration pathway. Spatially explicit projections of exposure to more frequent inland floods (of 1% AEP magnitude) were developed by integrating data from 29 global climate models (GCMs) under RCP8.5 and RCP4.5 in the mid- (2040–2059) and late- (2080–2099) 21st century with county-specific projections of U.S. populations for 2050 and 2090. Corresponding county- and state-level data are depicted in Figure 2 and Table S3, respectively. Populations are based on Integrated Climate and Land Use Scenarios (ICLUS) v2 county-level age group projections for the referenced year (i.e., 2050, 2090) (see Table S5 for corresponding projections holding population at 2010 levels and distribution).

widespread net increase in the number of people experiencing more frequent baseline 1% AEP floods, significant populations in some areas are projected to experience baseline 1% AEP floods less frequently (Figure 2).

Climate Change Impacts on the Magnitude of 1% AEP Flows

Like Figure 2, Figure 3 shows that the direction and magnitude of the anticipated changes in future 1% AEP flows compared with the baseline can vary substantially by county and region. Figure 3 shows a general trend of increasing flows in future 1% AEP events compared with the 2010 baseline over time, appearing as a shift to fewer blue-green shaded counties and more yellow-red shaded counties in 2090 than in 2050. Increases in flows for 1% AEP events projected in 2050 under both RCP4.5 and RCP8.5 are relatively and similarly small. By 2090, some increases in flows for the 1% AEP events are projected under RCP4.5; however, the anticipated increases in 1% AEP flows are far more pronounced under RCP8.5, particularly in California and southern Nevada. These areas have multiple counties that fall into the largest categories of change (i.e., having future 1% AEP flows >1.5 times the baseline).

The projected populations affected by changes in 1% AEP flows over time (Table 2) are largely consistent with the projected populations exposed to changes in 1% AEP flood frequency (Table 1) in terms of timing and distribution of the changes. More people live in counties that experience equal or larger 1% AEP flows in the future than smaller flows—in both 2050 and 2090, under both RCP4.5 and RCP8.5, and in almost every region. The only exceptions are the Midwest and Northeast regions for 2050 under the RCP4.5 scenario.

Increases in populations exposed to larger 1% AEP flows over time are more pronounced under RCP8.5 than under RCP4.5. Particularly striking is the increase in the number of people exposed to flows that are >1.5 times the size of the baseline 1% AEP flow under RCP8.5. Although almost no one is exposed to this high level of change in flow in 2050, roughly 51.3 million people of all ages are projected to live in counties that experience flows >1.5 times baseline levels in 2090, including nearly 5.4 million children ≤4 y old, and roughly 9.3 million persons ≥65 y old. This increase is almost entirely attributable to anticipated changes in the Southwest region, particularly in the heavily populated area of southern California (see Figure 3). Projections show that western regions, particularly California, western Washington, and the southwestern border of Texas, will see

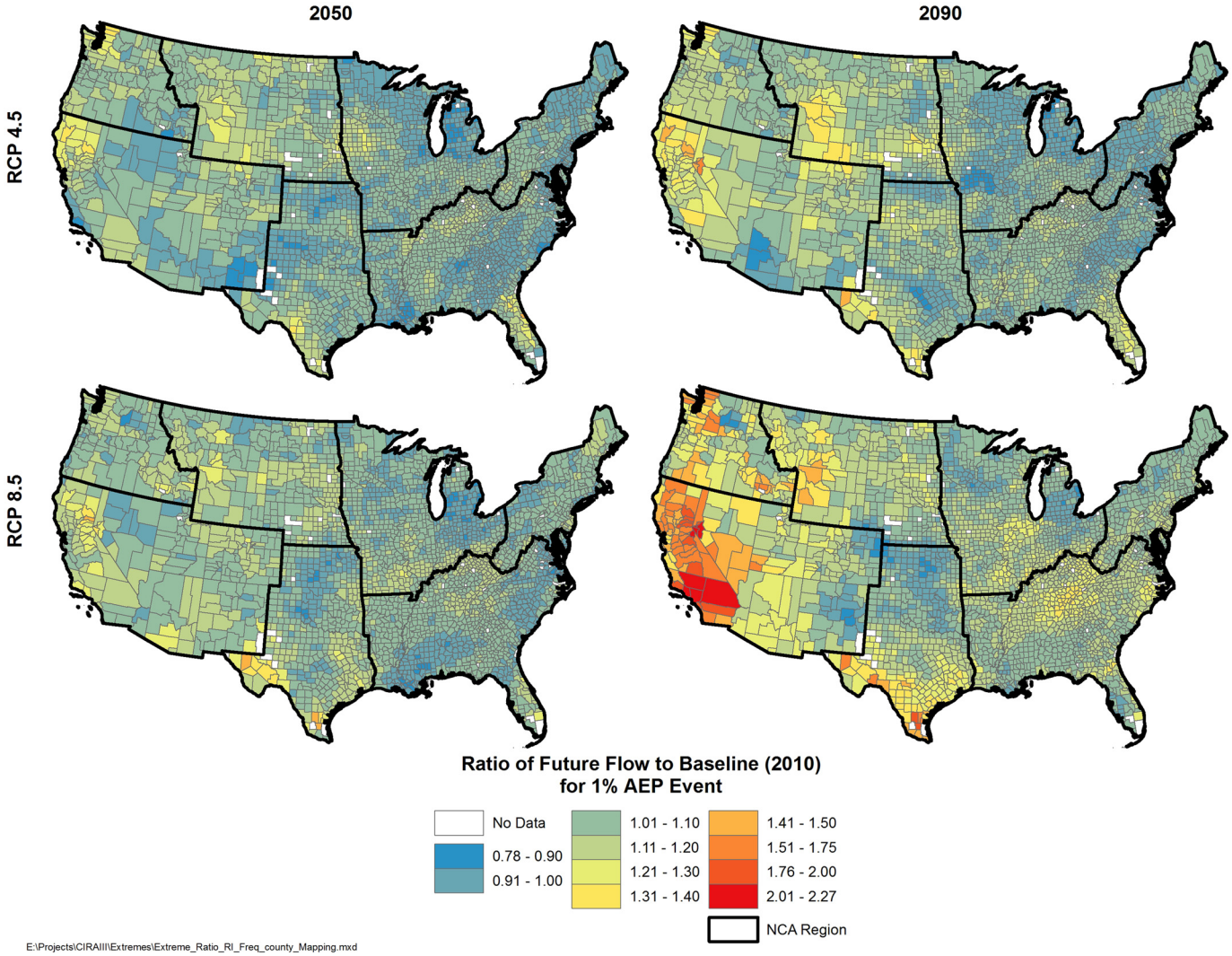

Figure 3. Projected change in the magnitude of baseline 1% annual exceedance probability (AEP) floods. Future county-level average future 1% AEP flow index (FFI_{100} ratios to the 2010 baseline 1% AEP flows are shown under RCP8.5 and RCP4.5 in 2050 and 2090. The most extreme increases in flow (values >1) are presented in dark red, and the largest reductions in flow (values <1) are presented in dark blue. RCP, representative concentration pathway.

Table 2. Populations affected by changes in the flow of baseline 1% AEP floods (millions of persons).

NCA region	Future flow more than 1.50 times larger than baseline			Future flow the same size to 1.50 times larger than baseline			Future flow smaller than baseline		
	Age 0–4	Age ≥65	All ages	Age 0–4	Age ≥65	All ages	Age 0–4	Age ≥65	All ages
RCP4.5 in 2050									
Northeast	0.00	0.00	0.00	2.43	4.88	25.58	3.76	8.06	40.19
Southeast	0.00	0.00	0.00	4.03	9.87	44.94	3.48	8.60	38.93
Midwest	0.00	0.00	0.00	3.14	6.04	33.35	3.46	6.78	36.32
Northern Great Plains	0.00	0.00	0.00	0.58	1.23	6.28	0.01	0.02	0.13
Southern Great Plains	0.00	0.00	0.00	3.65	7.74	37.33	0.65	1.48	6.99
Southwest	0.00	0.00	0.00	6.74	14.46	68.44	0.98	2.16	10.02
Northwest	0.00	0.00	0.00	1.21	2.69	13.09	0.07	0.14	0.70
Total	0.00	0.00	0.00	21.79	46.90	229.03	12.40	27.24	133.28
RCP4.5 in 2090									
Northeast	0.00	0.00	0.00	4.58	8.24	45.59	2.63	4.42	26.00
Southeast	0.00	0.00	0.00	6.64	12.92	67.43	2.51	5.21	25.97
Midwest	0.00	0.00	0.00	4.44	7.09	43.23	3.19	4.99	31.14
Northern Great Plains	0.00	0.00	0.00	0.69	1.25	7.01	0.04	0.05	0.35
Southern Great Plains	0.00	0.00	0.00	3.83	7.02	37.41	1.54	3.06	15.51
Southwest	0.02	0.12	0.31	8.71	16.07	84.52	0.98	1.84	9.58
Northwest	0.00	0.00	0.00	1.42	2.69	14.35	0.06	0.10	0.54
Total	0.02	0.12	0.31	30.30	55.28	299.53	10.94	19.67	109.09
RCP8.5 in 2050									
Northeast	0.00	0.00	0.00	4.85	10.21	51.58	1.34	2.73	14.19
Southeast	0.00	0.00	0.00	5.38	13.28	60.00	2.14	5.18	23.87
Midwest	0.00	0.00	0.00	3.86	7.72	40.87	2.74	5.10	28.80
Northern Great Plains	0.00	0.00	0.00	0.56	1.21	6.11	0.03	0.05	0.29
Southern Great Plains	0.00	0.00	0.00	4.01	8.56	41.26	0.28	0.65	3.07
Southwest	0.00	0.00	0.00	7.70	16.56	78.28	0.02	0.05	0.19
Northwest	0.00	0.00	0.00	1.23	2.74	13.31	0.05	0.09	0.48
Total	0.00	0.00	0.00	27.61	60.29	291.40	6.59	13.86	70.90
RCP8.5 in 2090									
Northeast	0.00	0.00	0.00	7.04	12.42	70.02	0.16	0.24	1.57
Southeast	0.00	0.00	0.00	8.68	17.10	88.52	0.46	1.03	4.87
Midwest	0.00	0.00	0.00	5.68	8.87	55.12	1.94	3.21	19.24
Northern Great Plains	0.00	0.00	0.00	0.67	1.16	6.71	0.06	0.13	0.66
Southern Great Plains	0.02	0.03	0.21	4.85	9.07	47.59	0.50	0.97	5.11
Southwest	5.30	9.14	50.27	4.08	8.21	40.88	0.33	0.68	3.27
Northwest	0.09	0.15	0.87	1.35	2.59	13.72	0.03	0.05	0.30
Total	5.41	9.33	51.34	32.36	59.42	322.56	3.49	6.32	35.03

Note: AEP, annual exceedance probability; NCA, National Climate Assessment; RCP, representative concentration pathway. Spatially explicit projections of exposure to changes in flow (magnitude) of inland floods (of 1% AEP frequency) were developed by integrating data from 29 global climate models (GCMs) under RCP8.5 and RCP4.5 in the mid- (2040–2059) and late- (2080–2099) 21st century with county-specific projections of U.S. populations for 2050 and 2090. Corresponding county- and state-level data are depicted in Figure 3 and Table S4, respectively. Populations are based on Integrated Climate and Land Use Scenarios (ICLUS) v2 county-level age group projections for the referenced year (i.e., 2050, 2090) (see Table S6 for corresponding projections holding population at 2010 levels and distribution).

substantial increases in both the frequency and magnitude of these flooding events, especially under RCP8.5 in 2090. Under both climate scenario projections, fewer people will live in counties that experience smaller 1% AEP flows in 2090 compared with 2050 despite increasing population over time. Although not shown in Figure 3, Table 2 shows large increases in the populations exposed to flows ≤1.5 times baseline 1% AEP levels in the Northeast and Southeast, likely because of high population density in these regions (see Table S4 for state-level results).

Subtracting the number of children ≤4 y old projected to experience smaller flows in 2050 from the number of children projected to experience floods equal to or larger than the baseline, we find that a net total of 11.6 million more children live in counties that experience an increase in 1% AEP flow under RCP8.5 than under RCP4.5. Similarly, a total of 26.8 million more adults ≥65 y old live in counties that experience an increase in 1% AEP flow under RCP8.5 than under RCP4.5 in 2050. By 2090, the difference between net populations experiencing an increase in flood flow under RCP8.5 and RCP4.5 increases to 14.9 million children ≤4 y old but remains roughly at 2050 levels for adults ≥65 y old. In other words, 14.9 million young children and 26.7 million older adults would avoid increases from the baseline 1% AEP flow levels under RCP4.5 compared with RCP8.5 each year by the end of the century.

Climate-Attributable Impact of Flooding Exposure on Static Population

To provide context for the portion of these impacts due to climate change only, we projected populations affected by changes in the frequency and flow of baseline 1% AEP floods holding future populations to 2010 levels and distribution (see Tables S5 and S6). When compared with projections that account for projected changes in future populations (Tables 1 and 2), the same overall patterns can be seen—more people are exposed under RCP8.5 than RCP4.5, more people are exposed in 2090 than in 2050, and regional patterns are similar—though these values shift downwards compared to projections that consider future population growth and migration. Similarly, the number of people experiencing the most severe category of change (baseline 1% AEP floods occurring ≥2 times more frequently; future flow >1.5 times larger than the baseline) jumps dramatically in 2090 under RCP8.5, with the greatest impacts again projected to occur in the Southwest (see Tables S5 and S6).

Wildfire Impacts

As with the flooding projections, wildfire smoke exposure projections for RCP8.5 in 2090 reflect the greatest potential exposure, with substantial regional differences (see Table 3, Table S7, and

Table 3. Populations projected to be exposed to wildfire smoke (millions of persons).

NCA region	Wildfire smoke exposure 1–3 times out of 20 years			Wildfire smoke exposure 4–6 times out of 20 years			Wildfire smoke exposure 7 or more times out of 20 years		
	Age 0–4	Age ≥65	All ages	Age 0–4	Age ≥65	All ages	Age 0–4	Age ≥65	All ages
RCP4.5 in 2050									
Northeast	0.81	1.64	8.60	0.00	0.00	0.00	0.00	0.00	0.00
Southeast	0.39	0.95	4.32	0.00	0.00	0.00	0.00	0.00	0.00
Midwest	0.16	0.29	1.68	0.00	0.00	0.00	0.00	0.00	0.00
Northern Great Plains	0.12	0.33	1.40	0.00	0.00	0.02	0.00	0.00	0.00
Southern Great Plains	0.06	0.12	0.62	0.00	0.00	0.00	0.00	0.00	0.00
Southwest	0.78	2.31	8.89	0.07	0.21	0.77	0.00	0.01	0.03
Northwest	0.48	1.13	5.28	0.01	0.03	0.13	0.00	0.00	0.00
Total	2.81	6.77	30.79	0.08	0.25	0.92	0.00	0.01	0.03
RCP4.5 in 2090									
Northeast	0.60	0.96	5.89	0.00	0.00	0.00	0.00	0.00	0.00
Southeast	0.36	0.75	3.71	0.00	0.00	0.00	0.00	0.00	0.00
Midwest	0.14	0.16	1.32	0.00	0.00	0.00	0.00	0.00	0.00
Northern Great Plains	0.10	0.27	1.14	0.00	0.00	0.01	0.00	0.00	0.00
Southern Great Plains	0.08	0.15	0.76	0.00	0.00	0.00	0.00	0.00	0.00
Southwest	0.91	2.25	9.66	0.06	0.17	0.66	0.00	0.00	0.01
Northwest	0.38	0.76	3.87	0.01	0.02	0.06	0.00	0.00	0.01
Total	2.58	5.29	26.36	0.07	0.19	0.74	0.00	0.00	0.01
RCP8.5 in 2050									
Northeast	0.82	1.69	8.75	0.00	0.01	0.03	0.00	0.00	0.00
Southeast	0.34	0.87	3.82	0.00	0.00	0.00	0.00	0.00	0.00
Midwest	0.20	0.35	2.10	0.00	0.00	0.00	0.00	0.00	0.00
Northern Great Plains	0.14	0.38	1.64	0.00	0.01	0.03	0.00	0.00	0.00
Southern Great Plains	0.04	0.07	0.37	0.00	0.00	0.00	0.00	0.00	0.00
Southwest	0.89	2.63	10.17	0.08	0.27	0.93	0.00	0.01	0.02
Northwest	0.61	1.43	6.71	0.01	0.04	0.15	0.00	0.00	0.00
Total	3.05	7.42	33.56	0.10	0.32	1.14	0.00	0.01	0.03
RCP8.5 in 2090									
Northeast	0.89	1.34	8.67	0.00	0.00	0.00	0.00	0.00	0.00
Southeast	0.92	1.85	9.43	0.00	0.00	0.01	0.00	0.00	0.00
Midwest	0.17	0.18	1.54	0.00	0.00	0.00	0.00	0.00	0.00
Northern Great Plains	0.11	0.27	1.18	0.00	0.01	0.04	0.00	0.00	0.00
Southern Great Plains	0.31	0.59	3.08	0.00	0.00	0.00	0.00	0.00	0.00
Southwest	0.91	2.16	9.50	0.10	0.28	1.13	0.00	0.01	0.04
Northwest	0.21	0.41	2.14	0.01	0.01	0.06	0.00	0.00	0.00
Total	3.52	6.82	35.53	0.11	0.31	1.24	0.00	0.01	0.05

Note: NCA, National Climate Assessment; RCP, representative concentration pathway. Spatially explicit projections of exposure to wildfire smoke were developed by integrating data from 5 global climate models (GCMs) under RCP8.5 and RCP4.5 in the mid- (2040–2059) and late- (2080–2099) 21st century with county-specific projections of U.S. populations for 2050 and 2090. Corresponding county- and state-level data are depicted in Figure 4 and Table S7, respectively, and county-level data for each GCM is shown in Figure S4. Populations are based on Integrated Climate and Land Use Scenarios (ICLUS) v2 county-level age group projections for the referenced year (i.e., 2050, 2090) (see Table S8 for corresponding projections holding population at 2010 levels and distribution).

Figure 4 for regional-, state-, and county-level projections, respectively). Our models estimate that tens of millions of people will be exposed to wildfire smoke in both time periods under both climate scenarios (Table 3). We project that three million more people are exposed to wildfire smoke in 2050 under RCP8.5 compared to RCP4.5; nearly 10 million more people are exposed in 2090 under RCP8.5 compared to RCP4.5. Ninety percent or more of persons in each affected age group are expected to experience wildfire smoke 1–3 times out of the 20-y time periods modeled. In contrast to the flooding results, the total projected population anticipated to experience wildfire smoke exposure does not consistently increase from 2050 to 2090; there may be fewer counties with projected smoke exposure in 2090 compared to 2050 under RCP4.5 (Figure 4) as the total affected population decreases from 2050 to 2090 by roughly 4.6 million persons (Table 3). Under RCP8.5, 2.1 million more people are exposed to wildfire smoke each year by 2090 compared to 2050; this estimate includes 0.5 million more children ≤4 y old but 0.6 million fewer adults ≥65 y old.

The Northeast and Southwest are projected to experience the highest populations exposed to wildfire smoke, with nearly 19 million people exposed 1–3 times between 2080 and 2099 in just these two regions under RCP8.5. While the population exposed to ≥7 wildfire years out of 20 is comparatively small (on the order of tens of thousands of people), they are almost all concentrated in the Southwest region. The region with the most dramatic increase in exposure from 2050 to 2090 under RCP8.5 is the Southeast.

While there is not a clear trend in the number of children or older adults exposed over time (from 2050 to 2090), fewer people in these vulnerable populations are exposed under RCP4.5 compared to RCP8.5 (Table 3). In 2050, 0.3 million more children ≤4 y old and 0.7 million more adults ≥65 y old are exposed under RCP8.5 than under RCP4.5. By 2090, 1.0 million more young children and 1.7 million more older adults are exposed under RCP8.5 than under RCP4.5. In other words, nearly 1 million young children and 1.7 million older adults would avoid exposure to wildfire smoke under RCP4.5 compared to RCP8.5 between 2080 and 2099.

Climate-Attributable Impact of Wildfire Smoke Exposure on Static Population

As with the flooding results, parallel patterns are observed when wildfire exposures are projected holding population size and distribution at 2010 levels (see Table S8). Specifically, larger populations are projected under the RCP8.5 scenario compared to the RCP4.5 scenario in both time periods and across all age groups and exposure categories. Similarly, projected wildfire smoke

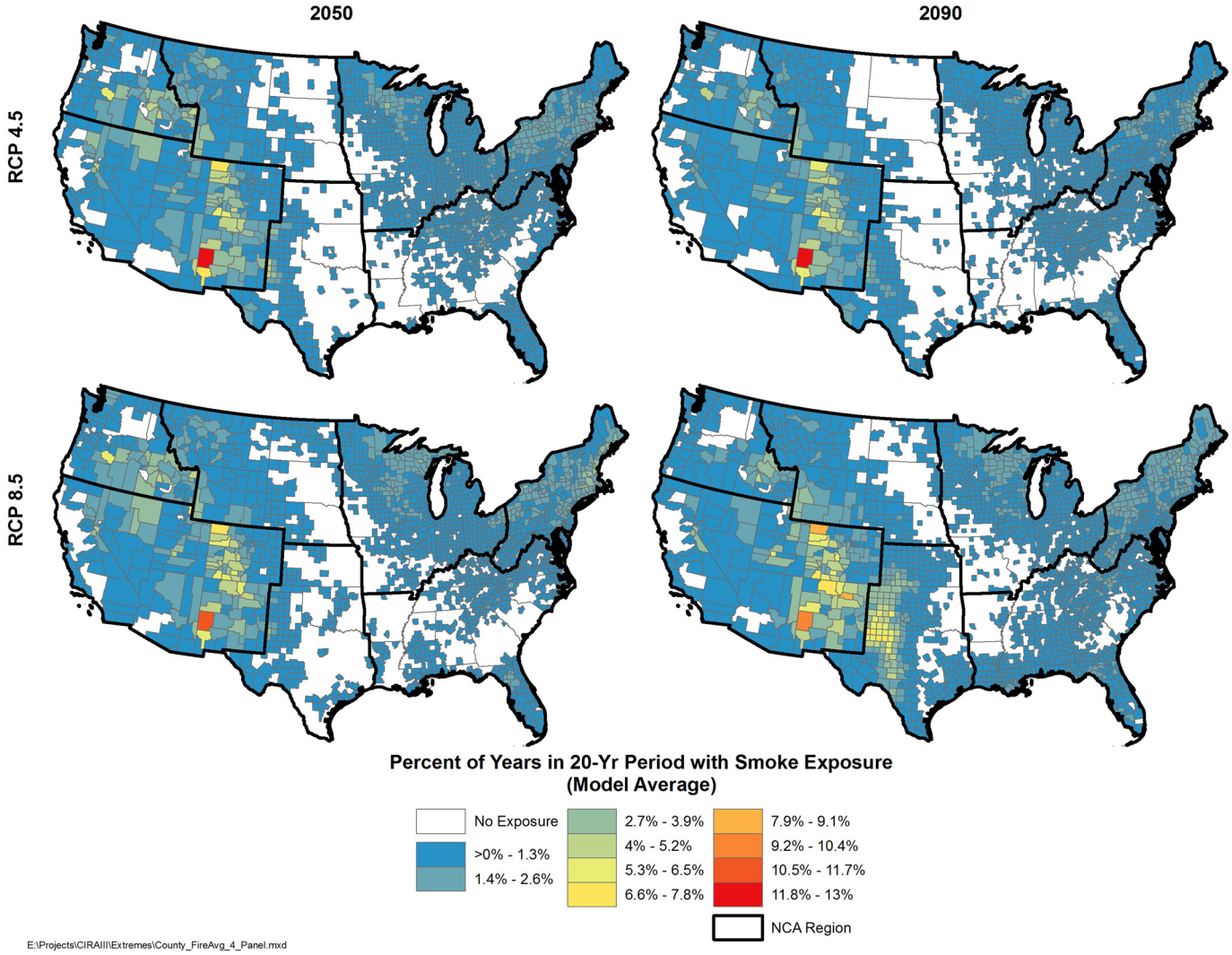

Figure 4. Projected percent of time counties will experience wildfire smoke. The projected years of exposure to wildfire smoke in MC2 cells where ≥6% of the cell area burns is expressed as a percentage of the total possible number of years of exposure from all MC2 cells in the county within future 20-y windows under RCP8.5 and RCP4.5 in 2050 and 2090. Values in deep red reflect the most frequent exposure to wildfire smoke, and dark blue values reflect the least frequent exposure. Counties with no projected wildfire smoke exposure are colored white. These counties either experienced >6% burning or were removed from consideration because 10% of all MC2 cells within the county are designated as agricultural or urban land. RCP, representative concentration pathway.

exposure is particularly pronounced the Northeast, Southeast, and Southwest regions across time periods and RCPs.

Discussion

In this study, we evaluated climate-related risks of exposure to public health threats in the United States from a subset of extreme weather events. Specifically, we integrated physical projections of inland flooding and wildfire smoke with age group–based population projections that account for population growth and movement. This approach addresses a need identified by Jurgilevich et al. (2017) for more modeling of exposure and vulnerability dynamics in climate risk analyses. Our results contribute to better understanding of the spatial patterns of future risk for vulnerable populations within and between U.S. regions and how the patterns compare under two different climate scenarios.

Under the climate scenarios and time periods considered, hundreds of millions of future CONUS residents of any age will be exposed to changes in future inland flooding that result in increased health risk each year, with tens of millions of those exposed being ≤4 y old or ≥65 y old. Millions of residents ≤4 y old or ≥65 y old, and tens of millions of residents of all ages will be exposed to wildfire smoke in the 20-y windows around 2050 and 2090. The projected populations exposed to the health stressors of inland flooding and wildfire smoke are consistently larger under RCP8.5 compared to RCP4.5 (Figure 5). The number of additional people exposed under RCP8.5 to increased measures of inland flooding compared to those exposed under RCP4.5 are roughly one third of the future total U.S. population in each age group. Importantly, many people will experience recurring exposure to flooding and wildfire hazards, which can lead to cumulative or compounding health impacts and weakening of adaptive capacity and resilience.

A benefit of the methods used in this study is the integration of the physical climate impacts with projected populations. In some instances, climate impacts are projected to be severe in a given region, but exposure is greater in a different region due to high population density. For instance, 2090 flooding impacts appear most severe for the Southwest region, primarily in California, in RCP8.5; however, the population-dense Northeast and Southeast are nearly equally affected. Digging deeper, we see that of the 50 million people exposed to future inland flooding flows that are

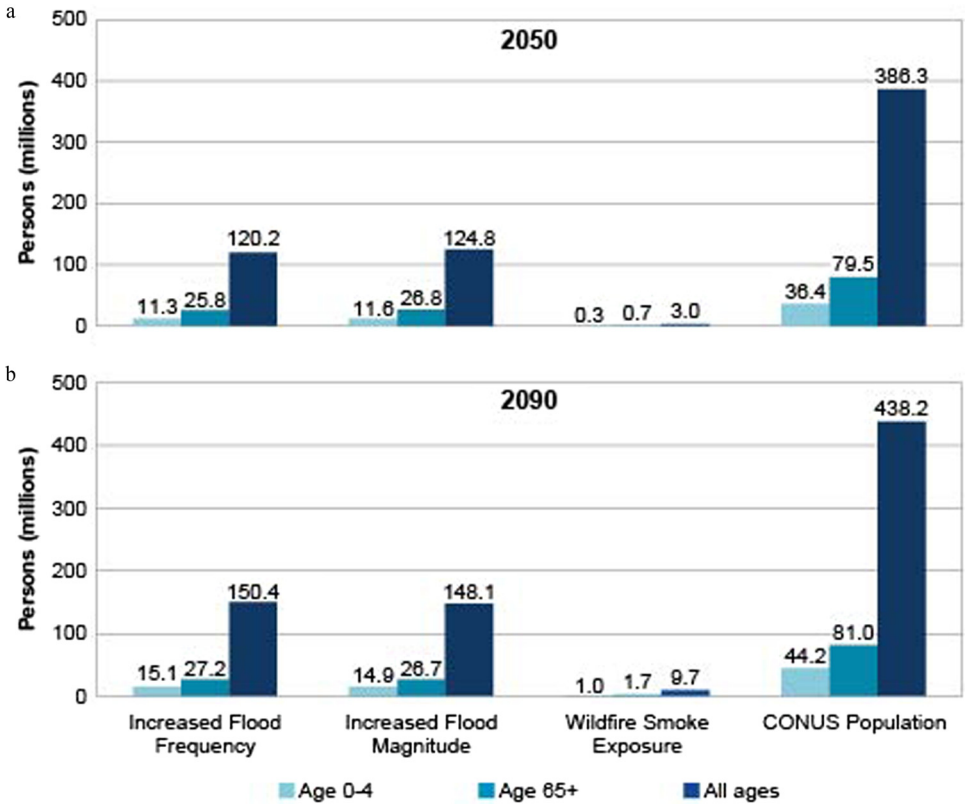

Figure 5. Avoided Exposure under RCP4.5. Difference in contiguous United States (CONUS) populations (in millions) exposed to modeled extreme events under RCP8.5 and RCP4.5 (values for RCP4.5 are subtracted from RCP8.5 values) for (*A*) 2050 and (*B*) 2090. The age group population living in an area exposed to a net increase in the frequency of the baseline 1% annual exceedance probability (AEP) flood ("Increased Flood Frequency") equals the population experiencing no change or an increase in the frequency of the baseline 1% AEP flood minus the population experiencing less frequent baseline 1% AEP floods. The age group population living in an area exposed to a net increase in the magnitude for future 1% AEP flows ("Increased Flood Magnitude") equals the population experiencing no change or an increase in the baseline 1% AEP flow minus the population experiencing a smaller flow. For context, "CONUS population" is the total population projected by ICLUSv2 in 2050 and 2090. RCP, representative concentration pathway.

≥1.5 times larger than baseline under RCP8.5 in 2090, 20 million are residents of Los Angeles County, an area that supports twice the number of people projected to reside in the entire Northern Great Plains region. These severe impacts in California are likely due to increases in the return period of extreme precipitation events, which are projected to occur more frequently even in regions like the Southwest, where total precipitation is expected to decline (Easterling et al. 2017). At the same time, arid regions with very low baseline 1% AEP flow levels require only small changes in future precipitation to lead to large threshold exceedances. By holding populations constant at 2010 levels, we confirm the critical role of the projected changes in climate in contributing to these increasing exposures.

In our methods, we attempted to limit the bias of any single GCM by aggregating and averaging results. Though a reasonable approach, this step has a dampening effect for extreme results at the tails of the impact distribution. Furthermore, we took conservative assumptions regarding impact exposure; different plausible assumptions could significantly affect results. For example, different assumptions about the average extent and direction of wildfire smoke could have a substantial impact on affected populations. Allowing burning in grid cells where >10% of the total MC2 cell area is classified as agricultural or urban land could increase the potential area burned by allowing fire to occur in the wildland–urban interface. In addition, if burning were to occur closer to urban areas, larger populations would experience smoke exposure under our approach. Furthermore, our methods do not capture the potential exposure associated with long-range transport of wildfire smoke that can travel hundreds (Luber et al. 2014) or even thousands (Morris et al. 2006) of miles from the source, as observed via satellites in the recent 2017 fires that burned in western states (NASA 2017). Such long-range transport, including from future wildfires in Mexico or Canada, would expose distant urban population centers to wildfire smoke (Dreessen et al. 2016; Heilman et al. 2014). Finally, though projections of climate change impacts on wildfires in Alaska demonstrate significant increases in the number of acres burned, particularly under RCP8.5 (Melvin et al. 2017), this study could not include Alaska exposure estimates as the LOCA downscaling was only available for the contiguous United States. Thus, our results very likely represent a lower bound for smoke exposure and show fewer U.S. residents affected by wildfire smoke than the recent work by Liu et al. (2016a, 2016b), who modeled some dispersion and transport, but only on a subnational basis and under one emissions scenario. Further limitations to the wildfire modeling approach can be found in U.S. EPA (2017a).

Other considerations that would affect exposure estimates include future adaptation, education or public health outreach programs, or general changes in land use and management, such as zoning and building codes that could reduce or mitigate potential future exposure to these hazards. For example, a current public education campaign around floodwaters communicates the message "Turn around, don't drown," which is aimed at discouraging contact with floodwaters, particularly by driving into them; this has been shown to be a critical factor in determining drowning deaths (NWS 2016). Adaptation measures, including increased freeboard requirements (elevation of a building's lowest floor), property

buyout programs, or abandonment, are likely to be taken in areas that experience recurring floods. Investments in flood protection could decrease overall exposure to these risks; however, a reasonable method for predicting floodplain protection in the future was beyond the scope of this analysis. These types of considerations, particularly as they relate to vulnerable populations like children and older adults, would be beneficial to address uncertainty when progressing from estimating changes in exposure to quantifying projected health outcomes (e.g., number of cases of illness, premature mortality) (Crimmins et al. 2016). Further limitations to the inland flooding modeling approach can be found in Wobus et al. (2017).

Our findings highlight regions with high numbers of exposed populations, particularly within vulnerable age groups, and potential areas of increased risk of exposure for recurring inland flooding and wildfire events. Both are important considerations for public health, disaster risk management, and climate adaptation planning and decision making. Such results can be used to identify areas that would benefit from regional risk assessments conducted at a finer scale (e.g., with current population estimates from the U.S. Census or projections generated by regional or state governments), which could inform adaptation needs and priorities for local policies.

Conclusion

Compared with future projections assuming moderate global emissions mitigation, millions of additional young children, older adults, and persons of all ages in the United States are projected to live in areas exposed to future inland flooding and wildfire smoke impacts under a high greenhouse gas emissions scenario. This represents a significant potential public health burden but also an opportunity to prevent exposures and prepare for adverse health outcomes associated with inland flooding and wildfires in the future.

Acknowledgments

The authors thank P. Morefield of the U.S. Environmental Protection Agency (U.S. EPA) for his advice with regard to the use of the Integrated Climate and Land Use Scenarios population data and J. Kim from the U.S. Forest Service for running the MC2 dynamic global vegetation model.

Financial support for this research was provided by the U.S. EPA through contract EP-BPA-12-H-0024 with Abt Associates Inc. The Oregon Department of Energy did not provide staff time or financial support for this research. The views expressed in this document are those of the authors and do not necessarily reflect those of their affiliated institutions including the U.S. EPA and the Oregon Department of Energy.

References

Al-Rousan TM, Rubenstein LM, Wallace RB. 2014. Preparedness for natural disasters among older US adults: a nationwide survey. Am J Public Health 104(3):506–511, PMID: 24432877, https://doi.org/10.2105/AJPH.2013.301559.

Bachelet D, Ferschweiler K, Sheehan TJ, Sleeter BM, Zhu Z. 2015. Projected carbon stocks in the conterminous USA with land use and variable fire regimes. Glob Chang Biol 21(12):4548–4560, PMID: 26207729, https://doi.org/10.1111/gcb.13048.

Bell JE, Brown CL, Conlon K, Herring S, Kunkel KE, Lawrimore J, et al. 2017. Changes in extreme events and the potential impacts on human health. J Air Waste Manag Assoc. PMID: 29186670, https://doi.org/10.1080/10962247.2017.1401017.

Bell JE, Herring SC, Jantarasami L, Adrianopoli C, Benedict K, Conlon K, et al. 2016. Impacts of extreme events on human health. In: *The Impacts of Climate Change on Human Health in the United States: A Scientific Assessment*. Crimmins A, Balbus J, Gamble JL, Beard CB, Bell JE, Dodgen D, eds, https://doi.org/10.7930/J0BZ63ZV.

Bell ML, Zanobetti A, Dominici F. 2013. Evidence on vulnerability and susceptibility to health risks associated with short-term exposure to particulate matter: a systematic review and meta-analysis. Am J Epidemiol 178(6):865–876, PMID: 23887042, https://doi.org/10.1093/aje/kwt090.

Bishop CH, Abramowitz G. 2013. Climate model dependence and the replicate Earth paradigm. Clim Dyn 41(3–4):885–900, https://doi.org/10.1007/s00382-012-1610-y.

Costello A, Abbas M, Allen A, Ball S, Bell S, Bellamy R, et al. 2009. Managing the health effects of climate change. Lancet 373(9676):1693–1733, PMID: 19447250, https://doi.org/10.1016/S0140-6736(09)60935-1.

Crimmins A, Balbus J, Gamble JL, Easterling DR, Ebi KL, Hess J, et al. 2016: Appendix 1: Technical support document: Modeling future climate impacts on human health. In: *The Impacts of Climate Change on Human Health in the United States: A Scientific Assessment*. Crimmins A, Balbus J, Gamble JL, Beard CB, Bell JE, Dodgen D, eds. Washington, DC:U.S. Global Change Research Program, https://doi.org/10.7930/J0KH0K83.

Cutter SL, Mitchell JT, Scott MS. 2000. Revealing the vulnerability of people and places: A case study of Georgetown County, South Carolina. Ann Assoc Am Geogr 90(4):713–737, https://doi.org/10.1111/0004-5608.00219.

Delfino RJ, Brummel S, Wu J, Stern H, Ostro B, Lipsett M, et al. 2009. The relationship of respiratory and cardiovascular hospital admissions to the southern California wildfires of 2003. Occup Environ Med 66(3):189–197, PMID: 19017694, https://doi.org/10.1136/oem.2008.041376.

Dreessen J, Sullivan J, Delgado R. 2016. Observations and impacts of transported Canadian wildfire smoke on ozone and aerosol air quality in the Maryland region on June 9–12, 2015. J Air Waste Manag Assoc 66(9):842–862, PMID: 26963934, https://doi.org/10.1080/10962247.2016.1161674.

Easterling DR, Arnold JR, Knutson T, Kunkel KE, LeGrande AN, Leung LR, et al. 2017. Precipitation change in the United States. In: *Climate Science Special Report: Fourth National Climate Assessment*, Vol. I. Wuebbles DJ, Fahey DW, Hibbard KA, Dokken DJ, Stewart BC, Maycock TK, eds. Washington, DC:U.S. Global Change Research Program, 275–307.

Ebi KL, Bowen K. 2016. Extreme events as sources of health vulnerability: Drought as an example. Weather Clim Extrem 11:95–102, https://doi.org/10.1016/j.wace.2015.10.001.

English PB, Richardson MJ. 2016. Components of population vulnerability and their relationship with climate-sensitive health threats. Curr Envir Health Rep 3(1):91–98, PMID: 26800675, https://doi.org/10.1007/s40572-016-0076-1.

FEMA (Federal Emergency Management Agency). 2017. Flood Zones. https://www.fema.gov/flood-zones [accessed 1 July 2017].

Gamble JL, Balbus J, Berger M, Bouye K, Campbell V, Chief K, et al. 2016. Populations of Concern. In: *The Impacts of Climate Change on Human Health in the United States: A Scientific Assessment*. Crimmins A, Balbus J, Gamble JL, Beard CB, Bell JE, Dodgen D, eds. Washington, DC:U.S. Global Change Research Program, https://doi.org/10.7930/J0Q81B0T.

Hantson S, Arneth A, Harrison SP, Kelley DI, Prentice IC, Rabin SS, et al. 2016. The status and challenge of global fire modelling. Biogeosciences 13(11):3359–3375, https://doi.org/10.5194/bg-13-3359-2016.

Haq G. 2017. Growing old in a changing climate. Public Policy Aging Rep 27(1):8–12, https://doi.org/10.1093/ppar/prw027.

Heilman WE, Liu Y, Urbanski S, Kovalev V, Mickler R. 2014. Wildland fire emissions, carbon, and climate: Plume rise, atmospheric transport, and chemistry processes. For Ecol Manage 317:70–79, https://doi.org/10.1016/j.foreco.2013.02.001.

Hollmann FW, Mulder TJ, Kallan JE. 2000. "Methodology and Assumptions for the Population Projections of the United States: 1999 to 2100." Population Division Working Paper No. 38. Washington, DC:U.S. Department of Commerce, Bureau of the Census, Population Division, Population Projections Branch. https://www.census.gov/population/www/documentation/twps0038/twps0038.html [accessed 1 July 2017].

Jurgilevich A, Räsänen F, Groundstroem F, Juhola S. 2017. A systematic review of dynamics in climate risk and vulnerability assessments. Environ Res Lett 12(1):013002, https://doi.org/10.1088/1748-9326/aa5508.

Knutti R, Abramowitz G, Collins M, Eyring V, Gleckler PJ, Hewitson B, Mearns L. 2010. Good practice guidance paper on assessing and combining multi model climate projections. In: *Meeting Report of the Intergovernmental Panel on Climate Change Expert Meeting on Assessing and Combining Multi Model Climate Projections*. Stocker TF, Qin D, Plattner GK, Tignor M, Midgley PM eds. Bern, Switzerland:IPCC Working Group I Technical Support Unit, University of Bern. http://www.ipcc-wg2.awi.de/guidancepaper/IPCC_EM_MME_GoodPracticeGuidancePaper.pdf [accessed 1 July 2017].

Liang X, Lettenmaier DP, Wood EF, Burges SJ. 1994. A simple hydrologically based model of land surface water and energy fluxes for general circulation models. J Geophys Res 99(D7):14415–14428, https://doi.org/10.1029/94JD00483.

Liu JC, Mickley LJ, Sulprizio MP, Dominici F, Yue X, Ebisu K, et al. 2016a. Particulate air pollution from wildfires in the Western US under climate change. Clim Change 138(3–4):655–666, PMID: 28642628, https://doi.org/10.1007/s10584-016-1762-6.

Liu JC, Mickley LJ, Sulprizio MP, Yue X, Peng RD, Dominici F, et al. 2016b. Future respiratory hospital admissions from wildfire smoke under climate change in the Western US. Environmental Research Letters 11(12):124018, https://doi.org/10.1088/1748-9326/11/12/124018.

Liu JC, Wilson A, Mickley LJ, Dominici F, Ebisu K, Wang Y, et al. 2017. Wildfire-specific fine particulate matter and risk of hospital admissions in urban and rural counties. Epidemiology 28(1):77–85, PMID: 27648592, https://doi.org/10.1097/EDE.0000000000000556.

Livneh B, Bohn T, Pierce D, Munoz-Arriola F, Nijssen B, Vose R, et al. 2015. A spatially comprehensive, hydrometeorological data set for Mexico, the U.S., and Southern Canada 1950–2013. Sci Data 2:150042, PMID: 26306206, https://doi.org/10.1038/sdata.2015.42.

Luber G, Knowlton K, Balbus J, Frumkin H, Hayden M, Hess J, et al. 2014. Human health. In: *Climate Change Impacts in the United States: The Third National Climate Assessment*, Melillo JM, Richmond TC, Yohe GW, eds. Washington, DC:U.S. Global Change Research Program, 220–256, https://doi.org/10.7930/J0PN93H5.

McKenzie D, Littell JS. 2017. Climate change and the eco- hydrology of fire: Will area burned increase in a warming western USA?. Ecol Appl. 27(1):26–36, PMID: 28001335, https://doi.org/10.1002/eap.1420.

Melillo JM, Richmond TC, Yohe GW, eds. 2014. Climate Change Impacts in the United States: The Third National Climate Assessment U.S. Global Change Research Program. Washington, DC:U.S. Government Printing Office, https://doi.org/10.7930/J0Z31WJ2.

Melvin AM, Murray J, Boehlert B, Martinich JA, Rennels L, Rupp TS. 2017. Estimating wildfire response costs in Alaska's changing climate. Clim Change 141(4):783–795, https://doi.org/10.1007/s10584-017-1923-2.

Meyer MA. 2017. Elderly perceptions of social capital and age-related disaster vulnerability. Disaster Med Public Health Prep 11(1):48–55, PMID: 27839520, https://doi.org/10.1017/dmp.2016.139.

Mizukami N, Clark M, Gutmann E, Mendoza P, Newman AJ, Nijssen B, et al. 2016. Implications of the methodological choices for hydrologic portrayals of climate change over the contiguous United States: Statistically downscaled forcing data and hydrologic models. J Hydrometeor 17(1): 73–98, https://doi.org/10.1175/JHM-D-14-0187.1.

Morris GA, Hersey S, Thompson AM, Pawson S, Nielsen JE, Colarco PR, et al. 2006. Alaskan and Canadian forest fires exacerbate ozone pollution over Houston, Texas, on 19 and 20 July 2004. J Geophys Res 111(D24):D24S03, https://doi.org/10.1029/2006JD007090.

NASA (National Aeronautics and Space Administration). 2017. Wildfire Smoke Crosses U.S. On Jet Stream. https://www.nasa.gov/image-feature/goddard/2017/wildfire-smoke-crosses-us-on-jet-stream [accessed 1 July 2017].

NWS (National Weather Service). 2016. Turn around don't drown PSA. http://www.nws.noaa.gov/os/water/tadd [accessed 24 July 2017].

OSU (Oregon State University). 2011. MC1 Dynamic Vegetation Model. http://www.fsl.orst.edu/dgvm/ [accessed 24 July 2017].

Patz JA, Frumkin H, Holloway T, Vimont DJ, Haines A. 2014. Climate change: challenges and opportunities for global health. JAMA 312(15):1565–1580, PMID: 25244362, https://doi.org/10.1001/jama.2014.13186.

Perera FP. 2017. Multiple threats to child health from fossil fuel combustion: impacts of air pollution and climate change. Environ Health Perspect 125(2):141–148, PMID: 27323709, https://doi.org/10.1289/EHP299.

Pierce DW, Cayan DR, Maurer EP, Abatzoglou JT, Hegewisch KC. 2015. Improved bias correction techniques for hydrological simulations of climate change. J Hydrometeor 16(6):2421–2442, https://doi.org/10.1175/JHM-D-14-0236.1.

Pierce DW, Cayan DR, Thrasher BL. 2014. Statistical downscaling using localized constructed analogs (LOCA). J Hydrometeor 15(6):2558–2585, https://doi.org/10.1175/JHM-D-14-0082.1.

Rappold AG, Reyes JM, Pouliot G, Cascio WE, Diaz-Sanchez D. 2017. Community vulnerability to health impacts of wildland fire smoke exposure. Environ Sci Technol 51(12):6674–6682, PMID: 28493694, https://doi.org/10.1021/acs.est.6b06200.

Reid CE, Brauer M, Johnston FH, Jerrett M, Balmes JR, Elliott CT. 2016. Critical review of health impacts of wildfire smoke exposure. Environ Health Perspect 124(9):1334–1343, PMID: 27082891, https://doi.org/10.1289/ehp.1409277.

Sanderson B, Knutti R, Caldwell P. 2015a. A representative democracy to reduce interdependency in a multimodel ensemble. J Clim 28(13):5171–5194, https://doi.org/10.1175/JCLI-D-14-00362.1.

Sanderson B, Knutti R, Caldwell P. 2015b. Addressing interdependency in a multimodel ensemble by interpolation of model properties. J Clim 28(13):5150–5170, https://doi.org/10.1175/JCLI-D-14-00361.1.

Taylor K, Stouffer RJ, Meehl GA. 2012. An overview of CMIP5 and the experiment design. Bull Amer Meteor Soc 93(4):485–498, https://doi.org/10.1175/BAMS-D-11-00094.1.

Tebaldi C, Knutti R. 2007. The use of the multi-model ensemble in probabilistic climate projections. Philos Trans A Math Phys Eng Sci 365(1857):2053–2075, PMID: 17569654, https://doi.org/10.1098/rsta.2007.2076.

Terti G, Ruin I, Anquetin S, Gourley JJ. 2017. A situation-based analysis of flash flood fatalities in the United States. Bull Amer Meteor Soc 98(2):333–345, https://doi.org/10.1175/BAMS-D-15-00276.1.

Trtanj J, Jantarasami L, Brunkard J, Collier T, Jacobs J, Lipp E, et al. 2016. Climate impacts on water-related illness. In: *The Impacts of Climate Change on Human Health in the United States: A Scientific Assessment*. Crimmins A, Balbus J, Gamble JL, Beard CB, Bell JE, Dodgen D, eds. Washington DC:U.S. Global Change Research Program, https://doi.org/10.7930/J03F4MH.

U.S. EPA (U.S. Environmental Protection Agency). 2017a. "Multi-model Framework for Quantitative Sectoral Impacts Analysis: A Technical Report for the Fourth National Climate Assessment." Washington, DC:U.S. Environmental Protection Agency https://cfpub.epa.gov/si/si_public_record_Report.cfm?dirEntryId=335095 [accessed 1 July 2017].

U.S. EPA. 2017b. "Updates to the Demographic and Spatial Allocation Models to Produce Integrated Climate and Land Use Scenarios (ICLUS) (Final Report, Version 2)." EPA/600/R-16/366F. Washington, DC:U.S. Environmental Protection Agency https://cfpub.epa.gov/ncea/iclus/recordisplay.cfm?deid=322479 [accessed 1 July 2017].

U.S. Department of the Interior, Bureau of Reclamation. 2016. Downscaled CMIP3 and CMIP5 climate and hydrology projections – addendum. Release of downscaled CMIP5 climate projections (LOCA) and comparison with preceding information. Last modified October 2016. http://gdo-dcp.ucllnl.org/downscaled_cmip_projections/dcpInterface.html [accessed 7 November 2016].

U.S. Reclamation. 2014. Downscaled CMIP3 and CMIP5 climate and hydrology projections: Release of hydrology projections, comparison with preceding information, and summary of user needs. Denver, CO:U.S. Department of the Interior, Bureau of Reclamation, Technical Services Center.

United Nations. 2015. *World Population Prospects: Key Findings & Advance Tables. The 2015 Revision*. New York, NY:United Nations, Department of Economic and Social Affairs, Population Division. https://esa.un.org/unpd/wpp/publications/files/key_findings_wpp_2015.pdf [accessed 1 July 2017].

USGCRP (U.S. Global Change Research Program). 2016. *The Impacts of Climate Change on Human Health in the United States: A Scientific Assessment*. Crimmins A, Balbus J, Gamble JL, Beard CB, Bell JE, Dodgen D, eds. Washington, DC:U.S. Global Change Research Program. https://doi.org/10.7930/J0R49NQX.

USGCRP. 2017a. *Climate Science Special Report: Fourth National Climate Assessment*, Volume I. Wuebbles DJ, Fahey DW, Hibbard KA, Dokken DJ, Stewart BC, Maycock TK. eds. Washington, DC:U.S. Global Change Research Program.

USGCRP (U.S. Global Change Research Program). 2017b. NCA4 Chapters. http://www.globalchange.gov/content/nca4-planning [accessed 20 June 2017].

Verner G, Schütte S, Knop J, Sankoh O, Sauerborn R. 2016. Health in climate change research from 1990 to 2014: Positive trend, but still underperforming. Glob Health Action 9(1):30723, PMID: 27339855, https://doi.org/10.3402/gha.v9.30723.

Viger RJ, Bock A. 2014. GIS features of the geospatial fabric for national hydrologic modeling. https://doi.org/10.5066/F7542KMD [accessed 1 July 2017].

Watts N, Adger WN, Agnolucci P, Blackstock J, Byass P, Cai W, et al. 2015. Health and climate change: policy responses to protect public health. Lancet 386(10006):1861–1914, PMID: 26111439, https://doi.org/10.1016/S0140-6736(15)60854-6.

Wehner MF, Arnold JR, Knutson T, Kunkel KE, LeGrande AN. 2017: Droughts, floods, and wildfires. In: *Climate Science Special Report: Fourth National Climate Assessment*, Volume I. Wuebbles DJ, Fahey DW, Hibbard KA, Dokken DJ, Stewart BC, Maycock TK. eds. Washington, DC:U.S. Global Change Research Program, https://doi.org/10.7930/J0CJ8BNN.

Wobus C, Gutmann E, Jones R, Rissing M, Mizukami N, Lorie M, et al. 2017. Climate change impacts on flood risk and asset damages within mapped "100 year" floodplains of the contiguous United States. Nat Hazards Earth Syst Sci 17(12):2199–2211, https://doi.org/10.5194/nhess-17-2199-2017.

Wood AW, Leung LR, Sridhar V, Lettenmaier DP. 2004. Hydrologic implications of dynamical and statistical approaches to downscaling climate model outputs. Clim Change 62(1–3):189–216, https://doi.org/10.1023/B:CLIM.0000013685.99609.9e.

Wood AW, Mizukami N. 2014. CMIP5 1/8th degree daily weather and VIC hydrology datasets for CONUS, NCAR final project report to USACE responses to climate change project (W26HM423495778), 32 pages.

Zahran S, Brody SD, Peacock WG, Vedlitz A, Grover H. 2008. Social vulnerability and the natural and built environment: A model of flood casualties in Texas. Disasters 32(4):537–560, PMID: 18435768, https://doi.org/10.1111/j.1467-7717.2008.01054.x.